

Electron-state effect induced by helical structure of metal nanowires formulated by path integrals in Riemann space

H. Kato* and H. Yashiro

Yamanashi University, Faculty of Engineering, 4-3-11 Takeda, Kofu, 400-8511 Yamanashi, Japan

(Received 28 July 2004; published 4 January 2005)

Thin nanowires of a metal have a multishell structure in which several deformed helical shells are stacked. The purpose of this paper is to give a perspective on the electron state in a helical nanowire based on the Riemann geometrical formulation of quantum mechanics within the continuum approximation of a wire. The helical configuration of atoms in the wires results in a sort of vector potential, and the electron state is modulated by the winding number and the shear modulus of the shell. The energy dispersion curve depends on the imbalance of the slide and distortion angles of the wire.

DOI: 10.1103/PhysRevB.71.033401

PACS number(s): 73.21.Hb, 02.40.Ky

Recently, quantized conductance at room temperature has been investigated through the metallic nanowires formed at the elongated point contact.¹⁻³ Especially, in the nanowire of gold, the relation between the conductance and the atomic configuration is clarified by the combination of the measurements of the conductance by the STM and the structure by the TEM.² At thin nanowires the existence of the Multi Helical Shell structure (MHS) is confirmed through these experiments,^{4,5} whose helical structure is enhanced as the diameter of a wire decreases. The same helical structure is also discussed regarding the wires of Ti,⁶ Pt,⁷ Pb, and Al.⁸ This structure is considered widely present at the metal wire. A shell in MHS is formed by the lattice with a shear strain, which affects the radius and pitch of the helix.⁴

A study about the electron state in a helical wire pointed out a possibility of shifts and crosses of the energy dispersion curve, which affect the channel number of the conductance.⁹ This discussion treats the effect of torsion around the wire axis but neglects the slide along the axis. One of the purposes of this paper is to propose a model about the electron state in a helical wire which is affected by both the torsion and slide along the wire axis. An electron motion in the crystal with a dislocation has been discussed by applying a Riemann geometrical formulation.¹⁰ Because of the similarity of the structure between the dislocation in a crystal and the helical wire, we apply a Riemann geometrical formulation to discuss the electron state in a helical wire.

We introduce the hypothesis that the electron state is expressed by a localized base even in a deformed wire. This localized base reduces to the Wannier basis when the deformation is relaxed. Then, the local motion of an electron from the i th site to the j th site is determined independently from the global structure of the wire and the motion is reduced to a free electron in a relaxed space without deformation. If we denote the location of the i th site in the deformed space by \mathbf{x}_i and ξ_i in the relaxed space, the transition matrix satisfies the relation $\langle \mathbf{x}_j(t_f) | \mathbf{x}_i(t_i) \rangle = \langle \xi_j(t_f) | \xi_i(t_i) \rangle$. Here, t_i and t_f are times to occupy the initial and final sites. Using continuum approximation to the sites, the motion of an electron in the potential U at the relaxed space is governed by a Lagrangian

$$L = \frac{m}{2} \left(\frac{d\xi}{dt} \right)^2 - U, \quad (1)$$

with an effective mass m . Here, the site index is abbreviated because of the continuum approximation. The potential U is introduced to entrap the electron in a wire, which is assumed to be the well potential given by

$$U(\xi) = \begin{cases} 0 & \text{(inside of the wire)} \\ \infty & \text{(outside of the wire)} \end{cases}. \quad (2)$$

If we use the rectangular coordinate, the transition matrix $G = \langle \xi(t_f) | \xi(t_i) \rangle$ is expressed in the path-integral formulation as follows:

$$G = \int \mathcal{D}\xi(t) \exp \left[\frac{i}{\hbar} \int_0^T L(\dot{\xi}, \xi) dt \right]. \quad (3)$$

Here, the symbol $\mathcal{D}\xi(t)$ stands for the path-integration and $T = t_f - t_i$. The motion of an electron is related to the square of infinitesimal distance $d\xi^2$. If the relation between $d\xi$ and $d\mathbf{x}$ is determined, the motion of an electron can be expressed by a quadratic form of displacement vector $d\mathbf{x}$ in a deformed space. This quadratic form is the fundamental form of Riemann geometry and is the starting point of its quantization.¹⁰

In Fig. 1, the outer shell with radius R (a), which is a component of the multi-shell structure, and its unfolding diagram (b) are shown. The helical shell is characterized by two angles, α_R and β_R . The slide along the z -axis is determined

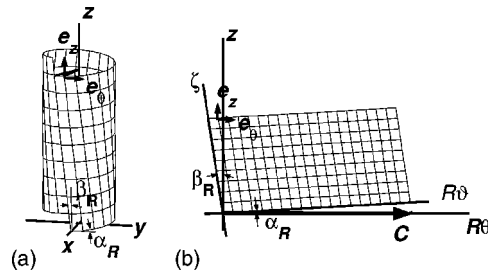


FIG. 1. A schematic diagram of the helical shell in a nanowire (a) and its unfolded diagram (b).

by angle α_R , which is related to the absolute value of the Burgers vector $b=2\pi R \tan \alpha_R$. The torsion around the z -axis is subjected by angle β_R , which determines the pitch of the helix $L_H=2\pi R/\tan \beta_R$. In Fig. 1(b), the length of the chiral vector is denoted by an arrow with a symbol C , whose size is measured along the circumference of a wire represented by $C=2\pi R=d \cos(\beta_R-\alpha_R)/\cos \beta_R$ with d as a size of the shell along the crystal lattice.⁴

Using the cylindrical coordinates, the relation between a displacement of an electron in a helical wire $d\mathbf{x}=(dr, d\theta, dz)$ and that in a relaxed space $d\xi=(dr, d\vartheta, d\zeta)$ is given by

$$d\xi = dr\mathbf{e}_r + (\cos \beta r d\theta + \sin \beta dz)\mathbf{e}_\theta / \cos \gamma \\ + (\cos \alpha dz - \sin \alpha r d\theta)\mathbf{e}_z / \cos \gamma, \quad (4)$$

where \mathbf{e}_r , \mathbf{e}_θ , and \mathbf{e}_z are unit vectors in the cylindrical coordinates, $\alpha=\alpha_R r/R$, $\beta=\beta_R r/R$, $\gamma=\beta-\alpha$. The transformation tensor B is defined by the following equation:

$$d\xi = (1+B) \cdot d\mathbf{x}. \quad (5)$$

Using relation (5) we transform the path of ξ into the path of \mathbf{x} in Eq. (3). For this transformation we need the Jacobian of functional¹⁰ $\mathcal{J}=\Pi_r \partial \xi(t)/\partial \mathbf{x}(t)$, which is given by

$$\mathcal{J} = \exp \left[- \int_{t_i}^{t_f} \dot{r} \frac{\partial}{\partial r} \text{tr}\{B\} dt \right]. \quad (6)$$

Then the Lagrangean L in Eq. (3) becomes as follows:

$$L = \frac{m}{2} \left[\dot{r}^2 + \frac{1}{\cos \gamma} \{ (\cos \beta r \dot{\theta} + \sin \beta \dot{z})^2 \right. \\ \left. + (\cos \alpha \dot{z} - \sin \alpha r \dot{\theta})^2 \right] - \frac{\hbar}{i} \dot{r} \frac{\partial}{\partial r} \text{tr}\{B\} - U - \Delta V_1. \quad (7)$$

Here, ΔV is a quantum correlation defined by

$$\Delta V_1 = - \frac{\hbar^2}{8m} \frac{1}{r^2}, \quad (8)$$

which is related to the Weyl ordering of operators in the cylindrical coordinates.^{11,12}

A classical Hamiltonian H_c of the system is obtained by the Legendre transformation on Eq. (7), whose explicit form is given by

$$H_c = \frac{1}{2m} \left[\left(p_r - \frac{\hbar}{i} \frac{\partial \text{tr}\{B\}}{\partial r} \right)^2 + \left(\cos \alpha \frac{p_\theta}{r} + \sin \alpha p_z \right)^2 \right. \\ \left. + \left(\cos \beta p_z - \sin \beta \frac{p_\theta}{r} \right)^2 \right] + U + \Delta V_1, \quad (9)$$

where p_r , p_θ , and p_z are momentums conjugate to r , θ , and z , respectively.

On the other hand, according to the procedure of quantization by use of the path-integral method,^{12,13} a quantum Hamiltonian which reduces to the Lagrangian (7) is obtained by the Weyl ordering of the classical Hamiltonian (9) with the momentum operators,

$$p_r = \frac{\hbar}{i} \left(\frac{\partial}{\partial r} + \frac{1}{r} + \frac{\gamma'}{2} \tan \gamma \right), \quad (10)$$

$$p_\theta = \frac{\hbar}{i} \frac{\partial}{\partial \theta}, \quad (11)$$

$$p_z = \frac{\hbar}{i} \frac{\partial}{\partial z}, \quad (12)$$

with $\gamma'=\gamma_R/R$, the quantum Hamiltonian H of an electron in a helical wire is given by

$$H = - \frac{\hbar^2}{2m} \left[\left(\frac{\partial}{\partial r} - \frac{\partial \text{tr}\{B\}}{\partial r} \right)^2 + \frac{\cos \alpha}{r} \left(\frac{\partial}{\partial r} - \frac{\partial \text{tr}\{B\}}{\partial r} \right) \right. \\ \left. + \left(\frac{\cos \alpha}{r} \frac{\partial}{\partial \theta} + \sin \alpha \frac{\partial}{\partial z} \right)^2 + \left(\cos \beta \frac{\partial}{\partial z} - \frac{\sin \alpha}{r} \frac{\partial}{\partial \theta} \right)^2 \right] + U \\ + \Delta V_1 - \Delta V_2. \quad (13)$$

Here, we use the Laplace-Beltrami operator in Riemann space at the Hamiltonian and introduce the quantum correction ΔV_2 due to the Weyl ordering, which is defined by

$$\Delta V_2 = - \frac{\hbar^2}{8m} \left[\left(\frac{1}{r} + \gamma' \tan \gamma \right)^2 - \frac{2}{r^2} + \frac{2\gamma'}{\cos^2 \gamma} \right]. \quad (14)$$

When $\alpha_R=0$ in the limit of small β_R , the Hamiltonian H given by Eq. (13) reduces to that given by Okamoto *et al.*⁹ When there is no torsion $\beta_R=0$ and up to the first order of α_R is considered, the Hamiltonian (13) results in

$$H = - \frac{\hbar^2}{2m} \left[p_r^2 + \left(\frac{p_\theta}{r} + \alpha p_z \right)^2 + p_z^2 \right] + U. \quad (15)$$

If the electron state is in an eigenstate along the z -axis and p_z can be regarded as a c -number, this Hamiltonian subjects the motion of an electron in the vector potential

$$\mathbf{A} = \frac{\alpha_R}{R} r^2 p_z \mathbf{e}_\theta. \quad (16)$$

This vector potential is equivalent to that of a uniform magnetic field and we can expect the Aharonov-Bohm effect on the motion around the circumference of a wire.

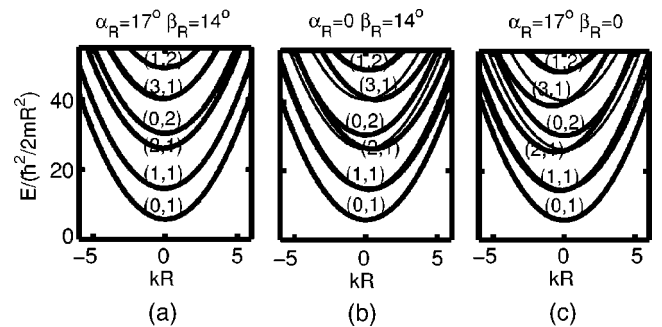


FIG. 2. Dispersion relation of the electron energy when $\alpha_R=17^\circ$ $\beta_R=14^\circ$ (a), $\alpha_R=0^\circ$ $\beta_R=14^\circ$ (b), and $\alpha_R=17^\circ$ $\beta_R=0^\circ$ (c). Thin curves for $\alpha_R=\beta_R=0^\circ$ are also depicted for the sake of comparison. The meaning of the indexes is discussed in the text.

If the wave function $\psi(r, \theta, z)$ is separated into $\psi(r, \theta, z) = \chi(r)e^{i(n\theta+kz)}$ with k as a wave number along the z -axis and n an integer (which is determined by the boundary condition about θ), the energy eigenvalue E is decided by the eigenvalue problem of the function $\chi(r)$:

$$\left(\frac{d}{dr} + a\right)^2 \chi + \left(\frac{1}{r} + \frac{\gamma'}{2} \tan \gamma\right) \left(\frac{d}{dr} + a\right) \chi + \frac{2Em}{\hbar^2} \chi - \left[\left(\cos \alpha \frac{n}{r} + \sin \alpha k\right)^2 + \left(-\sin \beta \frac{n}{r} + \cos \alpha k\right)^2 \right] \chi + \Delta V \chi = 0. \quad (17)$$

Here, $a = \partial \text{tr}\{B\} / \partial r$ and $\Delta V = \Delta V_1 - \Delta V_2$. Because of the well potential given by Eq. (2), the function $\chi(r)$ must satisfy the boundary conditions: $\lim_{r \rightarrow 0} r \chi'(R) = 0$ and $\chi(R) = 0$.

By means of numerical analysis on a discretized representation of Eq. (17), we obtain the eigenvalue of E and summarize it in Fig. 2. There are three cases where different values of α_R and β_R are given: (a) $\alpha_R = 17^\circ$, $\beta_R = 14^\circ$, (b) $\alpha_R = 0^\circ$, $\beta_R = 14^\circ$ and (c) $\alpha_R = 17^\circ$, $\beta_R = 0^\circ$. The thin curves are for the case of $\alpha_R = 0^\circ$ and $\beta_R = 0^\circ$, which are given for the sake of comparison. In Fig. 2(a), the solid and thin curves are almost aligned with each other and cannot be distinguished. This means that when the slide and the torsion are almost balanced $\alpha_R \approx \beta_R$, the energy dispersion is not affected by the helical structure except by the modulation on the reflection and transmission rates at wire terminals.

When the parameters α_R and β_R vanish, the function $\chi(r)$ reduces to $J_n(z_{np}r/R)$ where J_n is the Bessel function of n th order and z_{np} is its zero point, i.e., $J_n(z_{np}) = 0$ ($p = 1, 2, 3, \dots$). The index labeled for each curves in Fig. 2 is a pair of these numbers (n, p) . When there is an imbalance between the values of α_R and β_R ($\gamma_R \neq 0$), the dispersion relation shifts along the axis of the wave number k . The shift increases with the

value of the index n , so that a possible crossing will occur between the dispersion curves. As already discussed, if the Fermi level is located at this crossing point, the channel number of conduction will be affected.⁹ Even though the value of the reported γ_R or imbalance is small,⁴ the externally applied torsion involves a large imbalance and the electron state will be affected.

If the wire is composed of a single shell with radius R , the wave function becomes a two-dimensional function of θ and z and given by $\psi(\theta, z) = e^{i(n\theta+kz)}$ ($n = 0, 1, 2, \dots$). The energy eigenvalue E_{sh} of a two-dimensional electron on a shell is expressed by

$$E_{\text{sh}} = \frac{\hbar^2}{2mR^2} \left[\frac{n^2}{q_R} \cos^2 \gamma_R + q_R \left\{ kR - \frac{n}{q_R} \cos(\beta_R + \alpha_R) \sin \gamma_R \right\}^2 \right] \quad (18)$$

with $q_R = \sin^2 \alpha_R + \cos^2 \beta_R$. The electron state on a single helical shell is a one-dimensional wave which is quantized by an integer n and propagates along the wire axis with a wave number k . From Eq. (18), we can recognize that the dispersion curve shifts when α_R and β_R is imbalance or $\gamma_R \neq 0$ and its shift depends on the integer n . This dependence of the index n is similar to that appearing in Fig. 2 for a solidity wire.

In this paper we have given a model in which a helical structure of a nanowire is characterized by two parameters, the slide angle α_R and the torsion angle β_R , and the motion of an electron in a helically deformed wire is mapped onto a locally free motion in a space without the deformation. A global structure of a helical wire is taken into account on a Hamiltonian with an effective vector potential due to a helical curvature. According to this model, a possible shift and crossing of the energy dispersion curves is discussed, which depends on the imbalance of the angles α_R and β_R .

*Electronic address: katoh@yamanashi.ac.jp

¹J. I. Pascual, J. Méndez, J. Gómez-Herrero, A. M. Baró, N. García, and V. T. Binh, Phys. Rev. Lett. **71**, 1852 (1993).

²H. Ohnishi, Y. Kondo, and K. Takayanagi, Nature (London) **395**, 780 (1998).

³A. I. Yanson, G. R. Bollinger, H. E. van den Brom, N. Agrait, and J. M. van Ruitenbeek, Nature (London) **395**, 783 (1998).

⁴Y. Kondo and K. Takayanagi, Science **289**, 606 (2000).

⁵E. Tosatti and S. Prestipino, Science **289**, 561 (2000).

⁶B. Wang, S. Yin, G. Wang, and J. Zhao, J. Phys.: Condens. Matter **13**, L403 (2001).

⁷Y. Oshima, H. Koizumi, K. Mouri, H. Hirayama, K. Takayanagi,

and Y. Kondo, Phys. Rev. B **65**, 121401(R) (2002).

⁸O. Gülseren, F. Ercolessi, and E. Tosatti, Phys. Rev. Lett. **80**, 3775 (1998).

⁹M. Okamoto, T. Uda, and K. Takayanagi, Phys. Rev. B **64**, 033303 (2001).

¹⁰H. Araki, K. Kitahara, and K. Nakazato, Prog. Theor. Phys. **66**, 1895 (1981).

¹¹M. Omote, Nucl. Phys. B **120**, 325 (1977).

¹²C. Grosche and F. Stein, Z. Phys. C **36**, 699 (1987).

¹³C. Grosche and F. Stein, *Handbook of Feynman Path Integrals* (Springer-Verlag, Berlin 1998), p. 67.